RNAi-mediated gene silencing of vascular endothelial growth factor C suppresses growth and induces apoptosis in mouse breast cancer *in vitro* and *in vivo*

YONG-CHAO LIU[1,2*], WEN-HUI MA[1*], YIN-LIN GE[1], MEI-LAN XUE[1], ZHENG ZHANG[1], JIN-YU ZHANG[1], LIN HOU[1] and RUN-HONG MU[2]

[1]Department of Biochemistry and Molecular Biology, Medical College, Qingdao University, Qingdao, Shandong 266021; [2]Department of Immunology, Medical College, Beihua University, Jilin, Jilin 132013, P.R. China

Received July 7, 2015; Accepted August 19, 2016

DOI: 10.3892/ol.2016.5158

Abstract. Vascular endothelial cell growth factor (VEGF)-C promotes tumorigenesis by allowing lymph node metastasis and lymphangiogenesis, among other actions. RNA interference (RNAi) is a novel technique for suppressing target gene expression and may increase the effectiveness of cancer treatments. The present study assessed the influence of VEGF-C RNAi on the apoptosis and proliferation of mouse breast cancer cells *in vitro* and *in vivo*. A total of three pairs of small interfering RNA (siRNA) targeting mouse VEGF-C were designed and synthesized prior to transfection into 4T1 cells via a liposomal approach. Reverse transcription polymerase chain reaction, western blot analysis, a 3-(4,5-dimethylthiazol-2-yl)-2,5-diphenyltetrazolium bromide assay, Hoechst 33258 staining and flow cytometry were performed *in vitro* to analyze VEGF-C expression, cleaved caspase-3 protein expression and 4T1 cell proliferation and apoptosis. Experiments were also conducted *in vivo* on BALB/c mice with breast cancer. Tumor weight and volume were measured and the number of apoptotic cells in tumor tissues was assessed by a TUNEL assay. Immunohistochemical assays and an enzyme-linked immunosorbent assay were used to measure the expression of VEGF-C in tumor tissues. The results demonstrated that the three pairs of siRNA, particularly siV2, significantly reduced VEGF-C mRNA and protein levels in 4T1 cells. siV2 was deemed to be the most efficient siRNA and therefore was selected to be used in subsequent experiments. Furthermore, *in vitro* studies indicated that VEGF-C RNAi significantly decreased cell growth, induced apoptosis and upregulated the expression of cleaved caspase-3 protein. Tumor weight and volume in breast cancer *in vivo* models was reduced by the intratumoral injection of siV2. Antitumor efficacy was associated with decreased VEGF-C expression and increased induction of apoptosis. The present study therefore indicated that VEGF-C RNAi inhibited mouse breast cancer growth *in vitro* and *in vivo* and that it may be a novel targeted therapy for breast cancer.

Correspondence to: Professor Yin-Lin Ge, Department of Biochemistry and Molecular Biology, Medical College, Qingdao University, 38 Dengzhou Road, Qingdao, Shandong 266021, P.R. China
E-mail: geyinlin@126.com

*Contributed equally

Key words: small interfering RNA, RNA interference, vascular endothelial growth factor-C, apoptosis, breast cancer

Introduction

Breast cancer is one of the most common malignancies in female patients globally (1). Despite substantial advances in breast cancer diagnosis and treatment, the disease remains the second-leading cause of cancer-associated mortality among women in the USA (2). Although the precise mechanism of breast cancer progression is not fully understood, previous studies suggest that metastasis, which usually occurs in the regional lymph nodes preferentially as a first step, is a leading cause of mortality in patients with breast cancer (3,4). Thus, risk factors associated with lymph node metastasis, including vascular endothelial growth factor (VEGF)-C, have become the focus of a number of breast cancer studies.

VEGF-C, the primary promoter of lymphatic vessel formation, serves a critical role during embryogenesis, tumorigenesis and metastasis (5). Previously, it was considered that these effects were achieved by inducing the proliferation, migration and sprout formation of endothelial cells. This is due to the fact that VEGF-C functions by binding VEGF receptors (VEGFR) 3 and 2, which are primarily located on lymphatic and vascular endothelial cells, respectively (6,7). However, previous studies have demonstrated that VEGF-C and its receptors are present in certain tumor cells, including leukemic cells, gastric cancer cells and breast cancer cells (8-10), as well as endothelial cells, indicating that VEGF-C may facilitate tumor progression by directly acting on cancer cells.

The deregulation of apoptosis is also a representative characteristic of malignant tumor cells (11). In general, current therapeutic strategies for tumors aim to induce apoptosis (12).

Sun *et al* (13) demonstrated that VEGF-C RNA interference (RNAi), combined with epirubicin treatment, markedly decreased cell viability and increased apoptosis in the human breast cancer MCF-7 cell line. However, the majority of previous studies on the role of VEGF-C in breast cancer have focused on its role in lymphatic metastasis and lymphangiogenesis; the effect of VEGF-C on apoptosis remains to be fully elucidated. The present study aimed to identify the effects of targeting VEGF-C with small interfering RNA (siRNA) on the proliferation and apoptosis of mouse breast cancer 4T1 cells and to assess the influence of VEGF-C RNAi on breast cancer cell growth *in vivo*.

Materials and methods

Cell line and cell culture. The mouse breast cancer 4T1 cell line was acquired from the Shanghai Institutes for Biological Sciences of the Chinese Academy of Sciences (Shanghai, China). The 4T1 cells were routinely cultured in Dulbecco's modified Eagle's medium (DMEM; HyClone; GE Healthcare Life Sciences, Logan, UT, USA) containing 10% fetal bovine serum (HyClone; GE Healthcare Life Sciences) and 1% penicillin/streptomycin at 37˚C, in a humidified atmosphere containing 5% CO_2.

siRNA design and transfection. For RNAi, three 21-nucleotide siRNA duplexes targeting various regions encoding mouse VEGF-C (GenBank accession no., NM_009506) were designed using BLOCK-iT™ RNAi Designer (for siRNA) online software (https://rnaidesigner.thermofisher.com/rnaiexpress/setOption.do?designOption=sirna&pid=-5305478661531214507; Invitrogen; Thermo Fisher Scientific, Inc., Waltham, MA, USA). The nucleotide names and sequences were as follows: siV1 forward, 5'-CCACAAACACCUUCUUUAATT-3' and reverse, 5'-UUAAAGAAGGUGUUUGUGGTT-3'; siV2 forward, 5'-GCAAGACGUUGUUUGAAAUTT-3' and reverse, 5'-AUUUCAAACAACGUCUUGCTT-3'; and siV3 forward, 5'-GGAUGUUUACAGACAAGUUTT-3' and reverse, 5'-AACUUGUCUGUAAACAUCCTT-3'. To avoid triggering innate immune responses to the siRNA, the forward strands were 2'-O-methyl uridine modified, while the reverse strands were unmodified. A scrambled siRNA (SCR) with no homology to mouse genes was used as a negative control and its sequences were as follows: Forward, 5'-UUGAUGUGUUUAGUCGCUATT-3' and reverse, 5'-UAGCGACUAAACACAUCAATT-3'. To evaluate transfection efficiency, 3'-fluorescein amidite (FAM) fluorescence-labeled SCR was used. All siRNAs were chemically synthesized by Shanghai GenePharma Co. Ltd. (Shanghai, China).

The 4T1 cells were seeded into 6-well plates at a density of $1x10^5$ cells/well and incubated overnight at 37˚C until they reached 80% confluence. The cells were subsequently transfected with 100 nM siRNA using Hifectin II (Applygen Technologies, Inc., Beijing, China) according to the manufacturer's protocol. Once the 4T1 cells were growing exponentially they were divided into the following groups: Blank control group (BC group), negative control siRNA sequence transfection group (NC group), siV1 transfection group (siV1 group), siV2 transfection group (siV2 group) and siV3 transfection group (siV3 group). FAM-fluorescence detection was employed using the FAM-labeled SCR to evaluate transfection efficiency under an inverted fluorescence microscope (CKX41-F32FL; Olympus Corporation, Tokyo, Japan) 6 h following transfection. The follow-up procedures for all groups were identical: To determine the silencing effects of the various target sites, VEGF-C mRNA and protein levels were detected using reverse transcription-polymerase chain reaction (RT-PCR) and western blotting, respectively, 48 h subsequent to transfection. The siRNA sequence that exhibited the highest interference efficiency was then selected for additional experiments.

RT-PCR analysis. For the RT-PCR analysis, total RNA was isolated using TRIzol® reagent (Invitrogen; Thermo Fisher Scientific, Inc.) and cDNA was prepared with the GoScript™ Reverse Transcription System kit (Promega Corporation, Madison, WI, USA) according to the manufacturer's instructions. The primer design software Primer Premier version 5.0 (Premier Biosoft International, Palo Alto, CA, USA) was used to design the following primers: VEGF-C forward, 5'-GCCTAACATGCTTCGAGATC-3' and reverse, 5'-CTCATGGCTTTGTAGATGCC-3'; and β-actin forward, 5'-GGCATCGTGATGGACTCCG-3' and reverse, 5'-GTCGGAAGGTGGACAGCGA-3'. β-actin served as an internal reference. The primers were synthesized by Shanghai Sunny Biotech Co., Ltd. (Shanghai, China). PCR amplification was performed in a total reaction volume of 10 μl containing 5 μl PCR Mix buffer (Dongsheng Biotech Co., Ltd., Guangdong, China), 0.5 μl primer (50 pmol/μl), 0.5 μl downstream primer (50 pmol/μl), 3 μl water and 1 μl cDNA template. PCR reactions were performed as follows: 95˚C denaturation for 5 min; 30 cycles of 94˚C for 30 sec, 50˚C annealing for 30 sec and 72˚C for 1 min, with a final step at 72˚C for 5 min in a GeneAmp® PCR system 2400 Thermal Cycler (PerkinElmer, Inc., Waltham, MA, USA). Products were subjected to electrophoresis on a 2% agarose gel with ethidium bromide staining, followed by image capture using a Tanon 2500 Gel Imaging system (Tanon Science & Technology Co., Ltd., Shanghai, China).

Western blot analysis. Total protein was extracted from 4T1 cells using radioimmunoprecipitation assay buffer (Beyotime Institute of Biotechnology, Haimen, China) 48 h subsequent to transfection, and the level of protein was determined using the bicinchoninic acid assay. Equal amounts of protein lysates (50 μg) were separated by 5% sodium dodecyl sulphate-polyacrylamide gel electrophoresis and transferred to polyvinylidene difluoride membranes (EMD Millipore, Billerica, MA, USA). The membranes were blocked with 5% skimmed milk for 1 h and subsequently incubated at 4˚C overnight with polyclonal rabbit anti-mouse antibodies against VEGF-C (dilution, 1:100; catalog no., BA0548; Boster Bio-Engineering, Ltd., Co., Wuhan, China), β-actin (dilution, 1:300; catalog no., BA2305; Boster Bio-Engineering, Ltd., Co.) and caspase-3 (dilution, 1:200; catalog no., bs-0081R; Beijing Biosynthesis Biotechnology Co., Ltd., Beijing, China). The following day, membranes were washed with 1X Tris-buffered saline and Tween 20 (TBST) and incubated with the secondary horseradish peroxidase-labeled goat anti-rabbit antibody (catalog no., BA1054; Boster Bio-Engineering Ltd., Co.) diluted to 1:2,000 in skimmed milk/TBST for 1 h at room

temperature. The protein bands were visualized by enhanced chemiluminescence using SuperECL Plus kit (Applygen Technologies, Inc.) and band intensity was measured using Quantity One® software version 4.6.2 (Bio-Rad Laboratories, Inc., Hercules, CA, USA).

Cell viability assay. The 3-(4,5-dimethylthiazol-2-yl)-2,5-dip henyltetrazolium bromide (MTT) assay (Roche Diagnostics, Basel, Switzerland) was performed to evaluate the effect of VEGF-C interference on 4T1 cell proliferation. In brief, 4T1 cells were seeded onto 96-well plates at an optimal density of $3x10^3$ cells per well and incubated overnight at 37˚C, followed by transfection with 100 nM siV2 or 100 nM SCR. After 24, 48 and 72 h, cells were treated with 20 μl MTT (5 mg/ml) and cultures were re-incubated for an additional 4 h. Following removal of the supernatant, 150 μl dimethyl sulfoxide was added to each well to completely dissolve the crystals and absorbance was measured at 490 nm using a 2100C ELISA Reader (Rayto Life and Analytical Sciences Co., Ltd, Shenzhen, China).

Apoptotic cell morphology observation. The 4T1 cells were seeded into 24-well plates with glass slides on the bottom of the wells. Slides were washed gently with cold phosphate-buffered saline (PBS) 48 h subsequent to transfection. Cells were fixed by 4% paraformaldehyde for 1 h and washed 3 times with PBS. The resulting cells were stained with 0.5 ml Hoechst 33258 (10 μg/ml, Beyotime Institute of Biotechnology) at 37˚C for 10 min in the dark and the apoptotic features of cell death were established by measuring staining using fluorescence microscopy (Eclipse TS100; Nikon Corporation, Tokyo, Japan).

Flow cytometry. To analyze the rate of cell apoptosis, the Annexin V-fluorescein isothiocyanate (FITC) apoptosis detection kit was used (Invitrogen; Thermo Fisher Scientific, Inc.). Cells were harvested 48 h following transfection, washed twice with PBS and resuspended in 500 μl binding buffer. Cell suspensions were subsequently incubated with 5 μl Annexin V-FITC and 5 μl propidium iodide for 10 min at room temperature in the dark. The cells were evaluated immediately by flow cytometry (BD Biosciences, Franklin Lakes, NJ, USA). The results were quantified using winMDI 2.9 analysis software (The Scripps Institute Research Institute, Jupiter, FL, USA).

Animal models and experimental design. A total of 18 female BALB/c mice (4 weeks old; weighing 18-20 g) were purchased from the Shandong Laboratory Animal Center (Shandong, China) and were acclimated to laboratory conditions (26˚C, 50% humidity and 12 h day/night rhythm), with free access to food and water. The present study was approved by the Animal Ethics Committee of Medical College of Qingdao University (Qingdao, China). All experimental procedures were conducted in conformity with the National Institutes of Heath Guide for Care and Use of Laboratory Animals (14). The *in vivo* tumor generation assay was performed as previously described (15) with a minor modification: $5x10^4$ 4T1 cells suspended in 50 μl of DMEM were injected into the right-front dorsum of mice following acclimatization. Tumor size was measured every 2 days in two perpendicular dimensions (a=length, b=width) with a vernier caliper, and the size recorded as a volume (mm^3) as calculated by (axb^2)/2. When tumor values reached ~0.1 cm^3, mice were divided randomly into 3 groups (n=6 in each group). Mice were treated by intratumoral injection of either PBS, 1 μg/g body weight siV2 siRNA or 1 μg/g body weight SCR every 2 days. The siV2 or SCR was mixed with Hifectin II dissolved in PBS. All mice were sacrificed following 3 days subsequent to the 6th injection and their tumors were removed and weighed. Tumor sections were fixed in 4% formaldehyde for 48 h at 4˚C and subsequently embedded in paraffin and cut in 4 μm sections for immunohistochemical analysis.

Immunohistochemistry. Immunohistochemical analysis of VEGF-C was performed according to a procedure described previously (16). In brief, following deparaffinization with 100% xylene (Beijing Zhongshan Golden Bridge Biotechnology Co., Ltd., Beijing, China) and a graded alcohol series (80, 90 and 100%), rehydration with deionized water and antigen retrieval with citrate buffer (pH 6.0; Shanghai Weiao Biotechnology Co., Ltd., Shanghai, China), the tumor sections were incubated with rabbit anti-mouse polyclonal antibody against VEGF-C (dilution, 1:200) at 4˚C overnight. Following washing with PBS three times, the sections were incubated with biotinylated goat anti-rabbit secondary antibody (dilution, 1:1,000; catalog no., BA1003; Boster Bio-Engineering., Ltd., Co.) for 1 h at room temperature. Subsequent to being washed with PBS twice, the sections were stained with 3,3-diaminobenzidine solution using PV-6000-D kit (Beijing Zhongshan Golden Bridge Biotechnology Co., Ltd.) at room temperature for 5 min. Subsequently, the sections were counterstained with hematoxylin, coverslipped and observed under an optic microscope.

TUNEL assay for apoptotic cells. Apoptotic cell death in paraffin-embedded tumor tissue sections was examined using the TdT-FragEL™ DNA Fragmentation Detection kit (Calbiochem; EMD Millipore) according to the manufacturer's protocol. Apoptotic cells were identified as dark brown nuclei under a light microscope. The number of apoptotic cells was counted in 5 random fields (magnification, x400) in a blinded manner.

ELISA assays. A total of 100 mg tumor tissue from each sacrificed mouse from the various groups was ground with 200 ml cold PBS. Supernatants from the extract were subsequently collected and evaluated using an ELISA kit (USCN Life Science, Inc., Wuhan, China) to measure the protein concentration of VEGF-C according to the manufacturer's instructions. At the conclusion of the reaction, plates were read on the RT-2100C Microplate Reader (Rayto Life and Analytical Sciences Co., Ltd.). The results of the ELISA assay were expressed as pg/ml.

Statistical analysis. The data were expressed as the mean ± standard error. Results were analyzed by Student's *t*-test, using SPSS version 11.0 for Windows (SPSS, Inc., Chicago, IL, USA). All *in vitro* experiments were performed in triplicate. $P<0.05$ was considered to indicate a statistically significant difference.

Results

The transfection rate of siRNA. The intake of fluorescently labeled scrambled siRNA (100 nM) was observed using

fluorescence microscopy 6 h following transfection, in order to confirm the transfection efficiency of siRNA in 4T1 cells. The results demonstrated that transfection was highly efficient: >80% cells exhibited green fluorescence indicating the presence of fluorescent siRNA (Fig. 1).

Inhibitory effects of siRNA on the expression of VEGF-C in 4T1 cells. Cells were transfected with either 100 nM designed siRNA or 100 nM SCR, and 48 h following transfection the mRNA and protein expression of VEGF-C in 4T1 cells was estimated by RT-PCR and western blot analysis. As presented in Fig. 2A, VEGF-C mRNA expression levels in 4T1 cells transfected with siV1, siV2 and siV3 were 0.3180±0.0188, 0.1363±0.0132, 0.2700±0.0164, respectively, which was significantly decreased compared with the BC group (0.8563±0.0197; P<0.0001). Furthermore, the inhibition rate of siV2 was increased compared with that of siV1 and 3. VEGF-C mRNA expression did not significantly differ between BC and NC groups (P=0.0874). Similar results were observed regarding protein expression of VEGF-C. The levels of VEGF-C protein expression were significantly reduced in cells transfected with siV1 (0.1983±0.0157), siV2 (0.0740±0.0072) and siV3 (0.1997±0.0241), compared to BC group (0.7183±0.0279; P<0.0001, P<0.0001, and P<0.0001, respectively) and NC group (0.6750±0.0348; P=0.0002, P<0.0001, P=0.0004, respectively) (Fig. 2B). The results of RT-PCR and western blot analysis indicated that among the three siRNAs, siV2 exhibited a greater suppressive effect on VEGF-C compared with the other two siRNAs. Therefore, siV2 was selected for use in the subsequent experiments.

VEGF-C RNAi inhibits the proliferation of 4T1 cells. To quantify the influence of VEGF-C RNAi on 4T1 cell survival and growth, its effect on the proliferation of 4T1 cells following transfection was investigated. As presented in Fig. 3, cell proliferation was significantly attenuated by siV2 transfection in 4T1 cells compared to controls at 48 and 72 h following transfection (P=0.0047 and 0.0019, respectively). However, no significant difference was observed between the BC and NC groups at 48 and 72 h following transfection (P=0.0597 and 0.1635, respectively). These results suggest that specific VEGF-C silencing inhibits 4T1 cell survival and proliferation.

VEGF-C RNAi induces apoptosis of 4T1 cells. To investigate whether RNAi-induced attenuation of cell proliferation was attributable to the induction of apoptosis, the 4T1 cells were stained with Hoechst 33258 dye. As shown in Fig. 4A, the VEGF-C RNAi resulted in the induction of chromatin condensation and fragmentation within 4T1 cells, which could be visualized as intense pycnotic bluish-white fluorescence in the cell nuclei. Flow cytometry was subsequently performed to estimate the numbers of apoptotic cells (Fig. 4B). The apoptotic rate of cells in the siV2 group was 27.45±0.66% 48 h following transfection, which was significantly increased compared with that of the BC group (20.23±0.71%; P<0.001). No significant differences in the rate of apoptosis were detected between the NC (20.46±0.48%) and BC groups (P=0.8024).

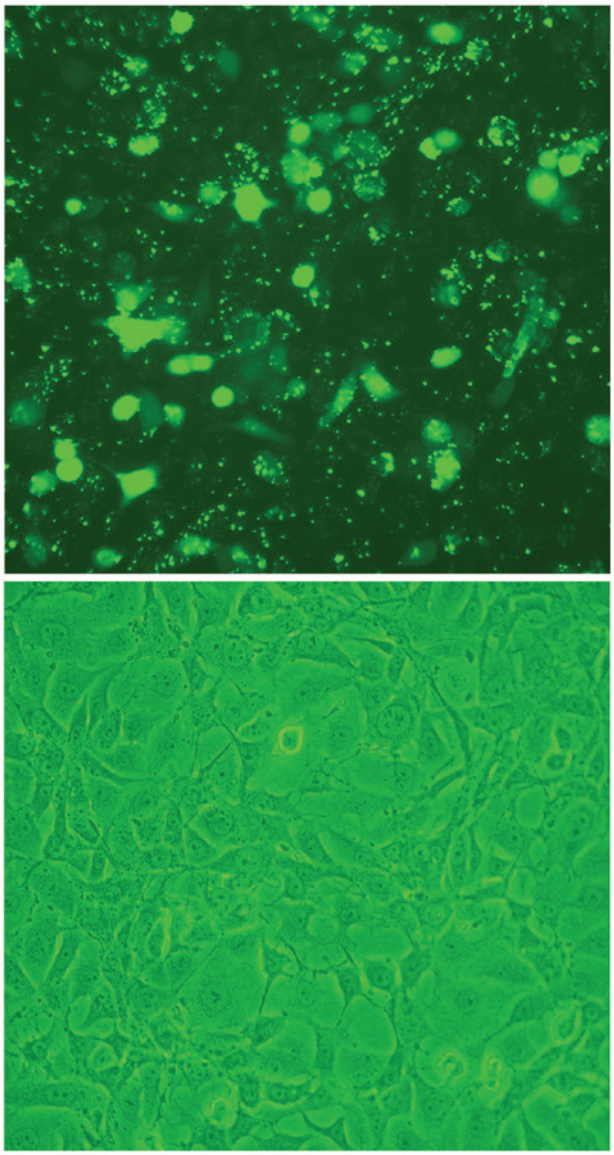

Figure 1. Assessment of siRNA transfection efficiency by fluorescence microscopy (magnification, x200), (A) Visualization of the cells under fluorescein-fluorescence light. (B) Visualization of the cells under normal light. Transfection efficiency with fluorescent siRNA (green) in 4T1 cells was identified as >80% 6 h post-transfection. siRNA, small interfering RNA.

VEGF-C RNAi upregulates caspase-3 cleavage. Activated caspase-3 is crucial for the induction of apoptosis. Therefore cleaved caspase-3 protein levels from 4T1 cells were measured by western blot analysis 48 h subsequent to transfection. The results indicated that siV2 transfection in 4T1 cells significantly increased caspase-3 cleavage compared with the controls (P=0.0009); however, no significant differences in cleaved caspase-3 protein expression were observed between the NC and BC groups (P=0.7181; Fig. 5). These data indicated that VEGF-C knockdown induces the caspase-3-dependent apoptotic signaling pathway in 4T1 cells.

VEGF-C RNAi suppresses 4T1 breast cancer growth in vivo. The data indicated that VEGF-C RNAi significantly inhibited 4T1 cell proliferation *in vitro*. To evaluate whether VEGF-C RNAi affects the proliferation of 4T1 cells *in vivo*, a tumorigenicity assay was performed in BALB/c mice. As shown in

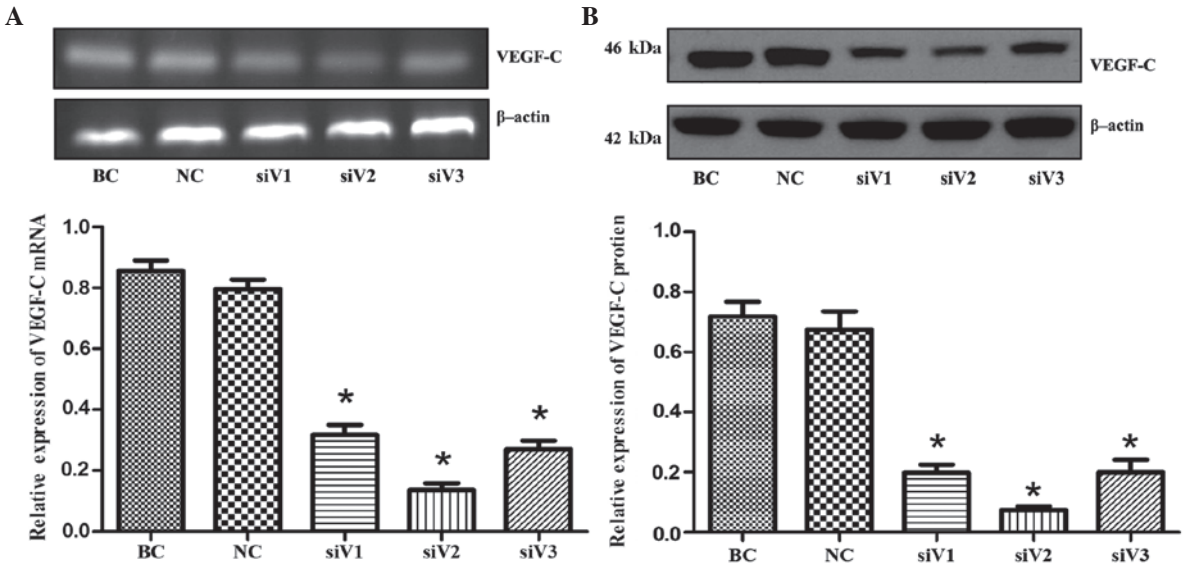

Figure 2. VEGF-C expression in 4T1 cells 48 h following transfection. (A) VEGF-C mRNA expression analysis in 4T1 cells by reverse transcription-polymerase chain reaction. (B) Western blot analysis of VEGF-C protein expression in 4T1 cells. β-actin in each lane served as an internal control for normalization. Data were expressed as the ratio of VEGF-C/β-actin expression. Mean values of triplicate assays ± standard deviation are presented. *P<0.05 vs. BC. VEGF-C, vascular endothelial growth factor C; BC, blank control; NC, negative control small interfering RNA sequence transfection group; siV1, siV1 transfection group; siV2, siV2 transfection group; siV3, siV3 transfection group.

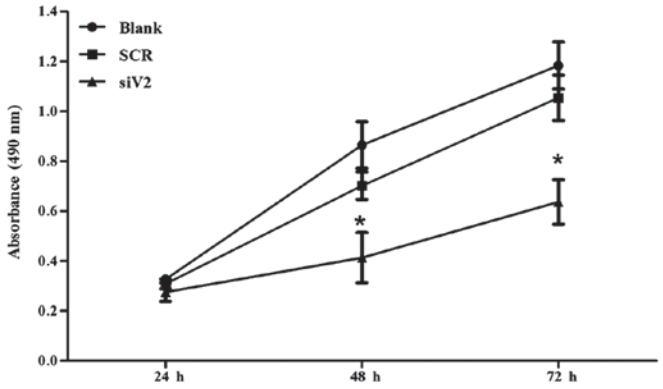

Figure 3. Influence of VEGF-C RNAi on the proliferation of 4T1 cells *in vitro*. The 4T1 cells were transfected with siV2 or SCR as a negative control for 24, 48 and 72 h, and measured for viability by the MTT assay. The vertical axis represents absorbance at 490 nm and the horizontal axis represents the time following transfection. Mean values of triplicate assays ± standard deviation are presented. *P<0.05 vs. blank control. RNAi, RNA interference; VEGF-C, vascular endothelial growth factor C; SCR, scrambled small interfering RNA group; siV2, siV2 transfection group; MTT, 3-(4,5-dimethylthiazol-2-yl)-2,5-diphenyltetrazolium bromide.

Fig. 6A, treatment with siV2 (1 μg/g body weight) resulted in a significant reduction in 4T1 cell tumor volume. Furthermore, the tumor weight of the siV2 group was significantly reduced compared with the BC group (P=0.0409), while there was no significant difference between that of NC group and BC group (P=0.9109; Fig. 6B).

VEGF-C RNAi induces apoptosis in tumor tissue. To confirm the ability of VEGF-C RNAi to induce apoptosis *in vivo*, *in situ* TUNEL staining was performed on sections of tumor tissue excised from 4T1 cell-implanted mice in each of the three groups. siV2 injection resulted in a significantly increased apoptosis rate compared with the BC (P=0.0342; Fig. 7). There were no significant differences between the NC and BC groups (P=0.8829). This indicates that VEGF-C RNAi may exert an antitumor effect on mouse breast cancer cells *in vivo*.

VEGF-C RNAi decreases the level of VEGF-C in tumor tissue. VEGF-C protein expression in isolated tumors from mice in various groups was examined by immunohistochemical staining and an ELISA assay. VEGF-C RNAi treatment resulted in a lower gross distribution of immunoreactive VEGF-C (yellow staining in cytoplasm or intercellular substance; Fig. 8A). Accordingly, the ELISA assay demonstrated that VEGF-C RNAi caused a significant reduction in intratumoral VEGF-C expression compared with the controls (P=0.0021; Fig. 8B).

Discussion

Since 2001, when Elbashir *et al* (17) successfully induced gene silencing in mammalian cells using synthetic 19-23-nucleotide double-stranded RNAs as siRNA, RNAi techniques have been widely used in the functional analysis of mammalian genes. The discovery of RNAi as a target-specific gene suppression technology has resulted in gene therapy becoming a promising novel treatment for various diseases, particularly for different types of cancer (18,19). The efficiency of siRNAs on the same target mRNA for different sequence sites typically varies. One critical precondition for RNAi is verifying an appropriate siRNA that efficiently knocks down the expression of target genes. Thus, several siRNAs are usually tested in order to select the most potent one (20,21). In the current study, three pairs of siRNAs targeting different sites of mouse VEGF-C mRNA were designed and transfected into 4T1 cells. Following transfection, relative mRNA and protein expression level analysis was performed, indicating that siV2 was the most efficient at

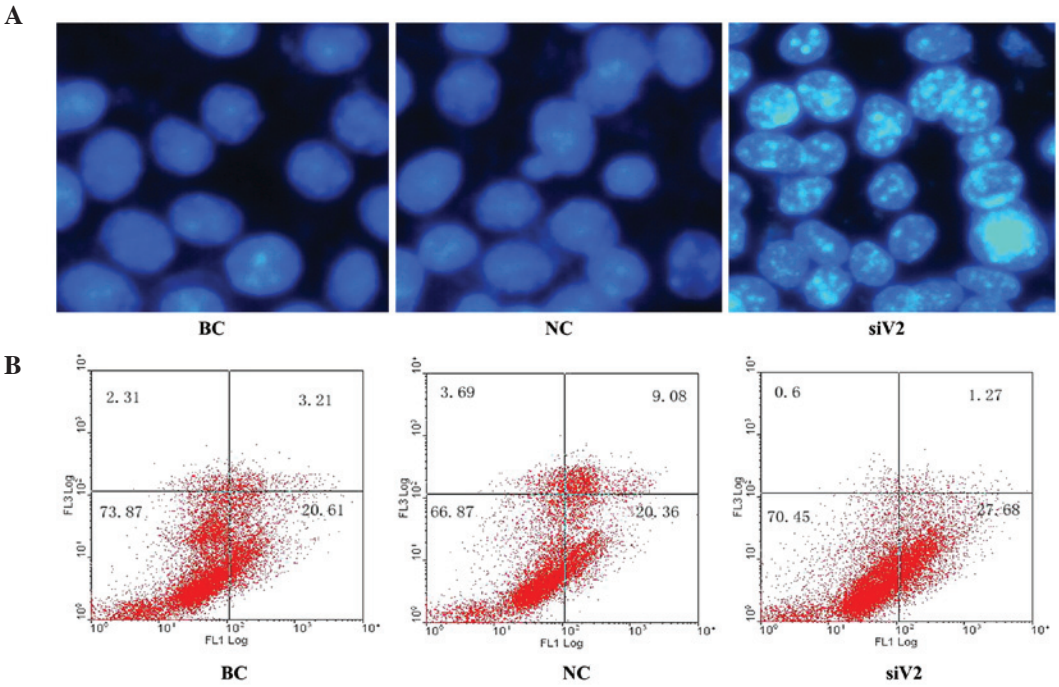

Figure 4. VEGF-C RNAi promotes apoptosis of 4T1 breast cancer cells *in vitro*. (A) Morphology of 4T1 cells 48 h subsequent to transfection observed under a fluorescence microscope (Hoechst 33258 staining; magnification, x400). (B) The apoptosis rate of 4T1 cells 48 h subsequent to transfection was determined by flow cytometry. The results are representative of three independent experiments. VEGF-C, vascular endothelial growth factor C; BC, blank control; NC, negative control small interfering RNA sequence transfection group; RNAi, RNA interference; siV2, siV2 transfection group.

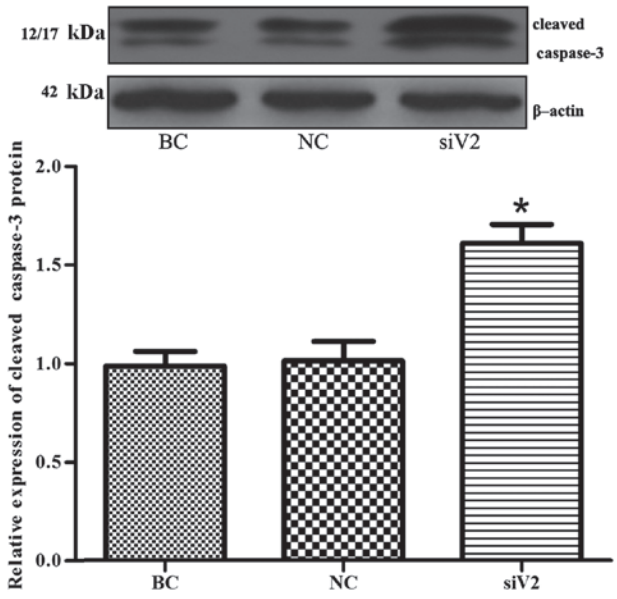

Figure 5. VEGF-C RNAi increases the level of cleaved caspase-3 protein in 4T1 cells. A total of 48 h following transfection, the expression of cleaved caspase-3 protein was analyzed by western blotting. β-actin in each lane served as an internal control for normalization. Data were expressed as the ratio of VEGF-C/β-actin expression. Data were confirmed in triplicate experiments and are presented as the mean ± standard error. *P<0.05 vs. BC. VEGF-C, vascular endothelial growth factor C; RNAi, RNA interference; BC, blank control; NC, negative control small interfering RNA sequence transfection group.

suppressing VEGF-C expression in 4T1 cells. The confirmation of an efficient siRNA targeting mouse VEGF-C in the current study lays the foundation for future research on VEGF-C.

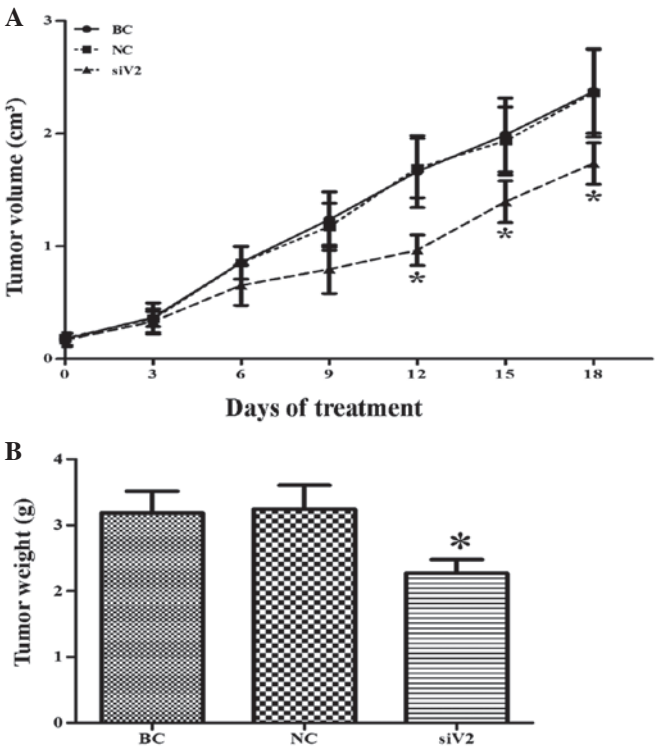

Figure 6. VEGF-C RNAi significantly inhibits tumor growth in 4T1 cell xenografts. (A) Tumor growth curves. Each point in the curve represents the mean ± SD (n=6). Therapy was initiated when tumor volume reached 0.1 cm^3. siV2 intratumoral injection inhibited tumor growth. *P<0.05 vs. BC group. (B) Weight of the tumors. Mean tumor weights were 3.185, 3.242 and 2.272 g, for the BC, NC and SiV2 groups, respectively. Each bar represents the mean ± SD (n=6). *P<0.05 vs. BC group. VEGF-C, vascular endothelial growth factor C; RNAi, RNA interference; BC, blank control; NC, negative control small interfering RNA sequence transfection group; siV2, siV2 transfection group; SD, standard deviation.

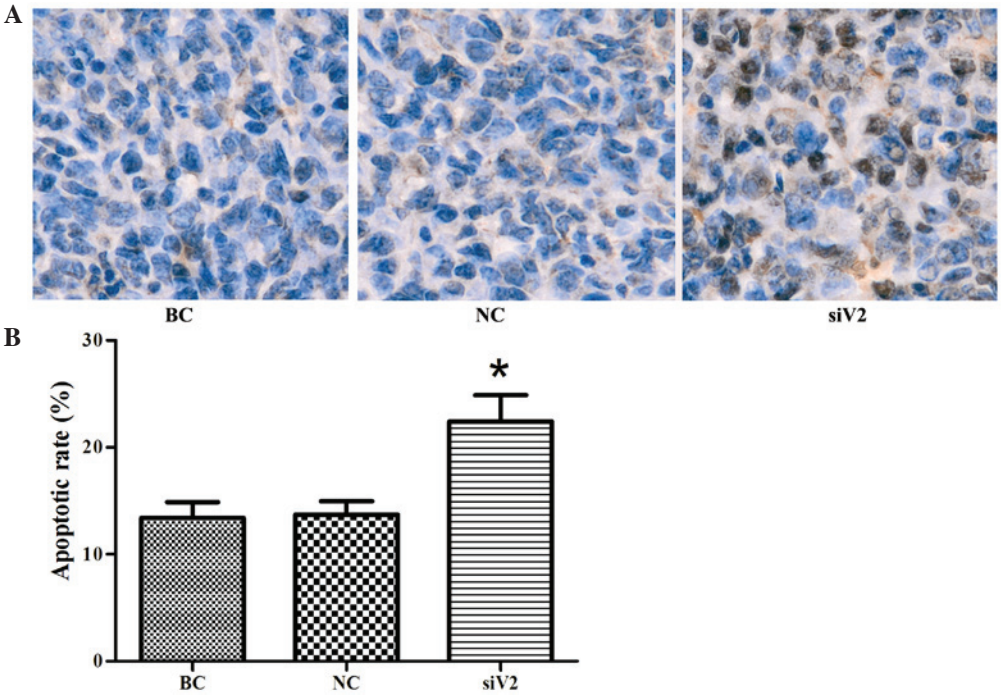

Figure 7. VEGF-C RNAi induces apoptosis *in vivo*. (A) Representative photographs of tumor sections examined by the TUNEL assay. TUNEL-positive cell nuclei (dark brown) were observed under an optical microscope (magnification, x400). (B) Graphs of the cell apoptotic rate. Data are presented as the mean ± standard deviation (n=6). *P<0.05 vs. BC group. VEGF-C, vascular endothelial growth factor C; RNAi, RNA interference; BC, blank control; NC, negative control small interfering RNA sequence transfection group; siV2, siV2 transfection group.

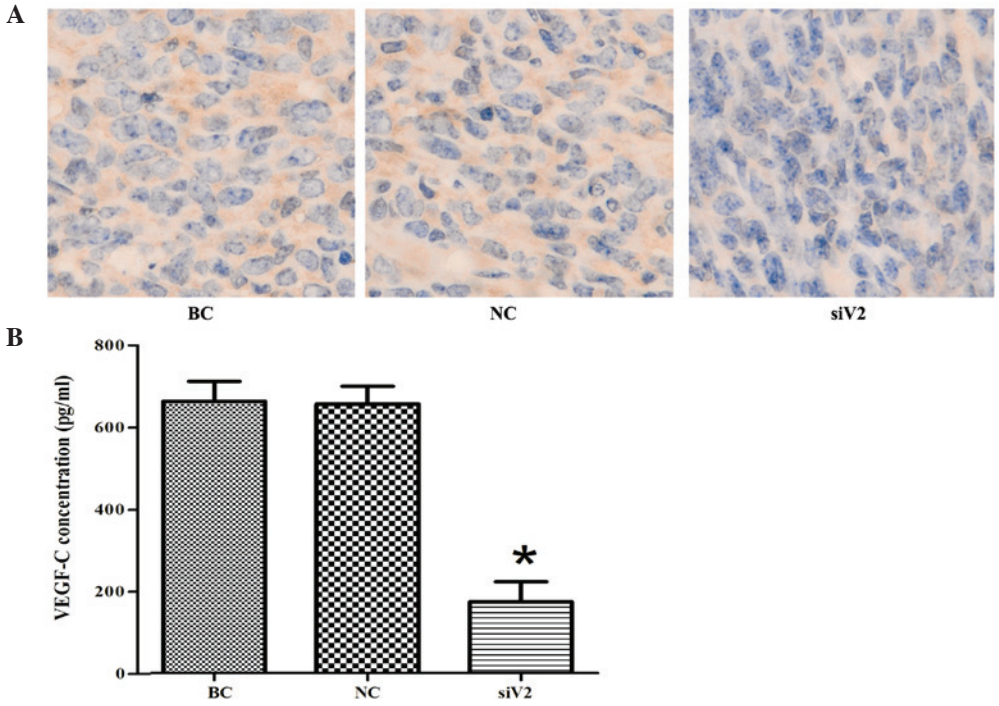

Figure 8. VEGF-C protein expression in excised tumors of various groups. (A) Representative photographs of the tumor sections examined by immunohistochemical staining for VEGF-C (magnification, x400). The assessment of VEGF-C expression was based on a cytoplasmic and intercellular substance-staining pattern. (B) Tumors were harvested and assayed for VEGF-C protein by an enzyme-linked immunosorbent assay. Each bar represents the mean ± standard deviation (n=6). *P<0.05 vs. BC group. VEGF-C, vascular endothelial growth factor C; RNAi, RNA interference; BC, blank control; NC, negative control small interfering RNA sequence transfection group; siV2, siV2 transfection group.

VEGF-C protein is part of the platelet-derived growth factor family and is a ligand for VEGFR-2 and VEGFR-3, which are broadly distributed on normal endothelial cells and certain human tumor cells (5,22,23). Studies using human or animal tumor models have demonstrated that malignant tumor cells secrete high levels of VEGF-C (22,24). Overexpression

of VEGF-C suggests a high degree of malignancy in breast cancer and poor patient prognosis (25). It has been demonstrated that an autocrine loop exists, by which VEGF-C stimulates tumor growth by directly stimulating tumor cells as well as acting on endothelial cells (8). However, the association between VEGF-C and tumor cell biological properties remains to be fully elucidated and is contested.

Tumor progression includes tumor cell proliferation, invasion, angiogenesis, the establishment of a metastatic niche, vascular intravasation and extravasation (26-28), any of which may affect tumor growth. Decio *et al* (29) suggested that VEGF-C promotes ovarian carcinoma progression through autocrine and paracrine mechanisms, while VEGF-C stimulates tumor growth *in vivo* but not *in vitro*. Zhang *et al* (30) concluded that VEGF-C enhanced the proliferation and invasiveness of bladder cancer T24 cells, suppressing apoptosis and facilitating migration, as well as upregulating p38 mitogen activated protein kinase and AKT phosphorylation. Muders *et al* (31) demonstrated that VEGF-C activated AKT-1/protein kinase B α, thus increasing prostate cancer cell proliferation during hydrogen peroxide stress. Using RNAi technology, a study by Feng *et al* (32) indicated that VEGF-C may attenuate non-small cell lung cancer progression: VEGF-C siRNA treatment downregulated the expression of VEGFR-2, VEGFR-3, CXCR4 and CCR7, and halted AKT, extracellular signal-related kinase and p38 signaling pathways *in vitro* and *in vivo*. All of the aforementioned analyses suggest that the VEGF-C autocrine effect activates a number of intracellular signaling pathways, which are critical for cellular growth and survival. Consequently, VEGF-C RNAi may directly inhibit the growth of breast cancer cells.

It is well known that tumor cells proliferate extensively. Previous studies have demonstrated that transfection of VEGF-C siRNA combined with epirubicin treatment or the downregulation of VEGFR-3 expression markedly decreases breast cancer cell viability *in vitro* (13,33). However, few studies have assessed the direct influence of VEGF-C on breast cancer cell proliferation and apoptosis. In the current study, it was demonstrated that silencing VEGF-C inhibited the proliferation of 4T1 cells *in vitro*. Furthermore, it was demonstrated that the knockdown of VEGF-C significantly increased the expression of cleaved capsase-3 and the cell apoptotic rate. Cell proliferation and apoptosis are associated with each other; imbalance between the amount of cell proliferation and apoptosis plays a critical role in the pathogenesis of cancer (34). Disturbance of apoptosis is a critical element in the pathogenesis of cancer and ultimately leads to cancer establishment and growth (35). Apoptosis is a biological process requiring the activation of several signaling cascades; caspase activation is one of the characteristic markers in the apoptotic process and caspase-3 is essential in inducing the nucleic changes associated with apoptosis (36). The results of the current study indicated that VEGF-C knockdown may trigger the apoptotic cascade of 4T1 cells and increase expression of cleaved caspase-3, resulting in increased apoptosis occurring in 4T1 cells. The decreased proliferation and increased apoptosis rate observed in 4T1 cells following treatment with VEGF-C siRNA demonstrates that VEGF-C serves a critical role in mouse breast cancer growth via an autocrine effect, although the precise mechanism remains to be elucidated.

Furthermore, the present study used a syngeneic female BALB/c mouse xenograft model of breast cancer to better evaluate the effects of VEGF-C siRNA *in vivo*. This immunocompetent BALB/c mouse model mimics the sequential stages of progression of human disease and reproduces the pattern of dissemination observed in patients (37,38). It was observed that intratumoral administration of VEGF-C siRNA significantly suppressed solid tumor growth, which was consistent with the conclusions of Xu *et al* (39) and Guo *et al* (40), who transfected VEGF-C siRNA into human breast cancer cells *in vitro* and *in vivo* by ultrasound-mediated or lentivirus-mediated methods, respectively. The current study also demonstrated that intratumoral administration of VEGF-C siRNA significantly increased the apoptotic rate of cells in tumor tissue. To the best of our knowledge, the present study is the first to demonstrate that the intratumoral administration of chemosynthetic VEGF-C targeting siRNA induces the apoptosis of breast cancer cells *in vivo*.

In conclusion, the findings of the present study suggest that VEGF-C RNAi markedly reduces cell growth and increases the apoptotic rate of breast cancer cells *in vitro* and *in vivo*. VEGF-C therefore may be developed as a novel treatment for breast cancer. However, the precise molecular mechanisms underlying the effects of VEGF-C RNAi on proliferation and apoptosis in 4T1 cells warrant further investigation.

Acknowledgements

The authors wish to thank Dr. Xueqin Wang and Dr. Zheng Zheng of the Biochemistry and Molecular Biology Department of Qingdao University Medical College (Qingdao, China) for their helpful comments and discussion on this study. The current study was supported by a grant from the Science and Technology Development Plan (2014) of Shandong Province (grant no. 2014GGH218023).

References

1. Montazeri A: Health-related quality of life in breast cancer patients: A bibliographic review of the literature from 1974 to 2007. J Exp Clin Cancer Res 27: 32, 2008.
2. Jemal A, Siegel R, Xu J and Ward E: Cancer statistics, 2010. CA Cancer J Clin 60: 277-300, 2010.
3. Nathanson SD: Insights into the mechanisms of lymph node metastasis. Cancer 98: 413-423, 2003.
4. Ran S, Volk L, Hall K and Flister MJ: Lymphangiogenesis and lymphatic metastasis in breast cancer. Pathophysiology 17: 229-251, 2010.
5. Joukov V, Kaipainen A, Jeltsch M, Pajusola K, Olofsson B, Kumar V, Eriksson U and Alitalo K: Vascular endothelial growth factors vegf-b and vegf-c. J Cell Physiol 173: 211-215, 1997.
6. Fournier E, Birnbaum D and Borg JP: Receptors for factors of the vegf (Vascular Endothelial Growth Family). Bull Cancer 84: 397-405, 1997.
7. Deckers MM, Karperien M, van der Bent C, Yamashita T, Papapoulos SE and Löwik CW: Expression of vascular endothelial growth factors and their receptors during osteoblast differentiation. Endocrinology 141: 1667-1674, 2000.
8. Su JL, Yen CJ, Chen PS, Chuang SE, Hong CC, Kuo IH, Chen HY, Hung MC and Kuo ML: The role of the VEGF-C/VEGFR-3 axis in cancer progression. Br J Cancer 96: 541-545, 2007.
9. Ge YL, Zhang X, Zhang JY, Hou L and Tian RH: The mechanisms on apoptosis by inhibiting VEGF expression in human breast cancer cells. Int Immunopharmacol 9: 389-395, 2009.
10. Kodama M, Kitadai Y, Tanaka M, Kuwai T, Tanaka S, Oue N, Yasui W and Chayama K: Vascular endothelial growth factor c stimulates progression of human gastric cancer via both autocrine and paracrine mechanisms. Clin Cancer Res 14: 7205-7214, 2008.

11. Kerr JF, Wyllie AH and Currie AR: Apoptosis: A basic biological phenomenon with wide-ranging implications in tissue kinetics. Br J Cancer 26: 239-257, 1972.
12. Hassan M, Watari H, AbuAlmaaty A, Ohba Y and Sakuragi N: Apoptosis and molecular targeting therapy in cancer. Biomed Res Int 2014: 150845, 2014.
13. Sun P, Gao J, Liu YL, Wei LW, Wu LP and Liu ZY: RNA interference (RNAi)-mediated vascular endothelial growth factor-C (VEGF-C) reduction interferes with lymphangiogenesis and enhances epirubicin sensitivity of breast cancer cells. Mol Cell Biochem 308: 161-168, 2008.
14. U.S. National Institutes of Health: Laboratory animal welfare: Public Health Service policy on humane care and use of laboratory animals by awardee institutions; notice. Fed Regist 50: 19584-19585, 1985.
15. Xue M, Ge Y, Zhang J, Liu Y, Wang Q, Hou L and Zheng Z: Fucoidan inhibited 4T1 mouse breast cancer cell growth in vivo and in vitro via downregulation of Wnt/β-catenin signaling. Nutr Cancer 65: 460-468, 2013.
16. Yan Y, Jia L, Zhang J, Liu Y and Bu X: Effect of recombinant Newcastle disease virus transfection on lung adenocarcinoma A549 cells in vitro. Oncol Lett 8: 2569-2576, 2014.
17. Elbashir SM, Lendeckel W and Tuschl T: RNA interference is mediated by 21- and 22-nucleotide RNAs. Genes Dev 15: 188-200, 2001.
18. Sioud M: RNA interference: Mechanisms, technical challenges, and therapeutic opportunities. Methods Mol Biol 1218: 1-15, 2015.
19. Mansoori B, Sandoghchian Shotorbani S and Baradaran B: RNA interference and its role in cancer therapy. Adv Pharm Bull 4: 313-321, 2014.
20. Li JP, Cao NX, Jiang RT, He SJ, Huang TM, Wu B, Chen DF, Ma P, Chen L, Zhou SF, *et al*: Knockdown of gcf2/lrrfip1 by rnai causes cell growth inhibition and increased apoptosis in human hepatoma HepG2 cells. Asian Pac J Cancer Prev 15: 2753-2758, 2014.
21. Pan XD, Yang ZP, Tang QL, Peng T, Zhang ZB, Zhou SG, Wang GX, He B and Zang LQ: Expression and function of GSTA1 in lung cancer cells. Asian Pac J Cancer Prev 15: 8631-8635, 2014.
22. Joukov V, Sorsa T, Kumar V, Jeltsch M, Claesson-Welsh L, Cao Y, Saksela O, Kalkkinen N and Alitalo K: Proteolytic processing regulates receptor specificity and activity of VEGF-C. Embo J 16: 3898-3911, 1997.
23. Joukov V, Pajusola K, Kaipainen A, Chilov D, Lahtinen I, Kukk E, Saksela O, Kalkkinen N and Alitalo K: A novel vascular endothelial growth factor, VEGF-C, is a ligand for the flt4 (VEGFR-3) and KDR (VEGFR-2) receptor tyrosine kinases. Embo J 15: 290-298, 1996.
24. Alitalo A and Detmar M: Interaction of tumor cells and lymphatic vessels in cancer progression. Oncogene 31: 4499-4508, 2012.
25. Kinoshita J, Kitamura K, Kabashima A, Saeki H, Tanaka S and Sugimachi K: Clinical significance of vascular endothelial growth factor-c (vegf-c) in breast cancer. Breast Cancer Res Treat 66: 159-164, 2001.
26. Chambers AF, Groom AC and MacDonald IC: Dissemination and growth of cancer cells in metastatic sites. Nat Rev Cancer 2: 563-572, 2002.
27. Duffy MJ, McGowan PM and Gallagher WM: Cancer invasion and metastasis: Changing views. J Pathol 214: 283-293, 2008.
28. Xu C, Gui Q, Chen W, Wu L, Sun W, Zhang N, Xu Q, Wang J and Fu X: Small interference RNA targeting tissue factor inhibits human lung adenocarcinoma growth in vitro and in vivo. J Exp Clin Cancer Res 30: 63, 2011.
29. Decio A, Taraboletti G, Patton V, Alzani R, Perego P, Fruscio R, Jürgensmeier JM, Giavazzi R and Belotti D: Vascular endothelial growth factor c promotes ovarian carcinoma progression through paracrine and autocrine mechanisms. Am J Pathol 184: 1050-1061, 2014.
30. Zhang HH, Qi F, Shi YR, Miao JG, Zhou M, He W, Chen MF, Li Y, Zu XB and Qi L: RNA interference-mediated vascular endothelial growth factor-C reduction suppresses malignant progression and enhances mitomycin C sensitivity of bladder cancer T24 cells. Cancer Biother Radiopharm 27: 291-298, 2012.
31. Muders MH, Zhang H, Wang E, Tindall DJ and Datta K: Vascular endothelial growth factor-C protects prostate cancer cells from oxidative stress by the activation of mammalian target of rapamycin complex-2 and AKT-1. Cancer Res 69: 6042-6048, 2009.
32. Feng Y, Hu J, Ma J, Feng K, Zhang X, Yang S, Wang W, Zhang J and Zhang Y: RNAi-mediated silencing of VEGF-C inhibits non-small cell lung cancer progression by simultaneously down-regulating the CXCR4, CCR7, VEGFR-2 and VEGFR-3-dependent axes-induced ERK, p38 and AKT signalling pathways. Eur J Cancer 47: 2353-2363, 2011.
33. Kurenova EV, Hunt DL, He D, Fu AD, Massoll NA, Golubovskaya VM, Garces CA and Cance WG: Vascular endothelial growth factor receptor-3 promotes breast cancer cell proliferation, motility and survival in vitro and tumor formation in vivo. Cell Cycle 8: 2266-2980, 2009.
34. Alison MR and Sarraf CE: Apoptosis: A gene-directed programme of cell death. J R Coll Physicians Lond 26: 25-35, 1992.
35. Desoize B and Sen S: Apoptosis or programmed cell death: Concepts, mechanisms and contribution in oncology. Bull Cancer 79: 413-425, 1992 (In French).
36. Snigdha S, Smith ED, Prieto GA and Cotman CW: Caspase-3 activation as a bifurcation point between plasticity and cell death. Neurosci Bull 28: 14-24, 2012.
37. Aslakson CJ and Miller FR: Selective events in the metastatic process defined by analysis of the sequential dissemination of subpopulations of a mouse mammary tumor. Cancer Res 52: 1399-1405, 1992.
38. Tao K, Fang M, Alroy J and Sahagian GG: Imagable 4T1 model for the study of late stage breast cancer. BMC Cancer 8: 228, 2008.
39. Xu Q, Sun T, Tian H, Wang C and Zhou H: Ultrasound-mediated vascular endothelial growth factor C (VEGF-C) gene microbubble transfection inhibits growth of MCF-7 breast cancer cells. Oncol Res 20: 297-301, 2013.
40. Guo B, Zhang Y, Luo G, Li L and Zhang J: Lentivirus-mediated small interfering RNA targeting VEGF-C inhibited tumor lymphangiogenesis and growth in breast carcinoma. Anat Rec (Hoboken) 292: 633-639, 2009.